CORROSION SCIENCE AND TECHNOLOGY, Vol.20, No.4(2021), pp.183~188
[Research Article]
pISSN 1598-6462 / eISSN 2288-6524
DOI: https://doi.org/10.14773/cst.2021.20.4.183

Electrochemical Characteristics of Synthesized Nb_2O_5-Li_3VO_4 Composites as Li Storage Materials

Youngmo Yang, Hyungeun Seo, and Jae-Hun Kim†

School of Materials Science and Engineering, Kookmin University, Seoul 02707, Republic of Korea
(Received July 28, 2021; Revised July 28, 2021; Accepted July 29, 2021)

The increasing demand for energy storage in mobile electronic devices and electric vehicles has emphasized the importance of electrochemical energy storage devices such as Li-ion batteries (LIBs) and supercapacitors. For reversible Li storage, alternative anode materials are actively being developed. In this study, we designed and fabricated an Nb_2O_5-Li_3VO_4 composite for use as an anode material in LIBs and hybrid supercapacitors. Nb_2O_5 powders were dissolved into a solution and the precursors were precipitated onto Li_3VO_4 through a simple, low-temperature hydrothermal reaction. The annealing process yielded an Nb_2O_5-Li_3VO_4 composite that was characterized by X-ray diffraction, electron microscopy, and X-ray photoelectron spectroscopy. Electrochemical tests revealed that the Nb_2O_5-Li_3VO_4 composite electrode demonstrated increased capacities of approximately 350 and 140 mAh g^{-1} at 0.1 and 5 C, respectively, were maintained up to 1000 cycles. The reversible capacity and rate capability of the composite electrode were enhanced compared to those of pure Nb_2O_5-based electrodes. These results can be attributed to the microstructure design of the synthesized composite material.

Keywords: *Niobium pentoxide, Li_3VO_4, Lithium storage, Electrode, Electrochemical properties*

1. Introduction

Recently, the importance of electrochemical energy storage devices is increasing with the rapid development of mobile electronic devices and electric vehicles. Among these devices, Li-ion batteries (LIBs) are predominantly used in the current market because of their high energy density, long cycle life, and reasonable cost [1-3]. Carbon-based materials such as graphite are commercially used as anode (negative electrode) materials in LIBs. Features such as moderate capacity (372 mAh g^{-1} for Li_6C phases), low reaction potential, and great cycle performance make graphite suitable for commercial LIBs [1,4]. However, current commercial applications of LIBs require them to have several other properties. Therefore, researchers have been actively pursuing alternative anode materials to replace graphite. In order to increase specific capacity, Li alloy-based materials such as Si and Sn have been widely investigated [5]. Furthermore, alternative intercalation-based materials such as $Li_4Ti_5O_{12}$, TiO_2, and Nb_2O_5 have been examined to enhance the rate capability (fast charging and high power) and safety features [6-8].

These materials exhibit relatively good rate performance; therefore, they can also be used in hybrid supercapacitors and Li-ion capacitors (LICs), wherein the aforementioned battery-type materials are employed for anodes and activated carbon materials are used for cathodes. Both LIB and LIC applications require intercalation-type materials to further improve the capacity and rate capability. Of these materials, niobium pentoxide (Nb_2O_5) materials have recently attracted significant attention as high-rate anodes because they are naturally abundant and can provide moderate capacity (~200 mAh g^{-1}) as well as excellent rate performance through a pseudocapacitive intercalation mechanism [9]. However, the current market demands increased reversible capacity while maintaining the rate performance.

In this study, we designed and synthesized an Nb_2O_5-Li_3VO_4 composite material to enhance the reversible capacity for electrochemical Li storage. Li_3VO_4 has garnered great interest as an intercalation-based anode material [10]. Its capacity of 397 mAh g^{-1} ($Li_{3+x}VO_4$, x = 2) is relatively higher than those of graphite and Nb_2O_5. Another benefit of this material is the high mobility of Li

†Corresponding author: jaehunkim@kookmin.ac.kr
Youngmo Yang and Hyungeun Seo: Graduate student, Jae-Hun Kim: Professor

ions; therefore, Nb_2O_5 was designed to be dispersed within the Li_3VO_4 matrix. The composite was synthesized by first dissolving the Nb_2O_5 powders into a solution and then precipitating the precursors onto Li_3VO_4 through a simple, low-temperature hydrothermal reaction. The resulting Nb_2O_5-Li_3VO_4 composite was characterized using several analytical tools. Electrochemical tests revealed that the composite electrode exhibits an increased capacity of approximately 350 mAh g^{-1} at 0.1 C, which is higher than that of Nb_2O_5 materials. Moreover, the capacity of about 140 mAh g^{-1} was maintained well without fading for up to 1000 cycles at a high rate of 5 C.

2. Experimental Methods

2.1 Material synthesis

Nb_2O_5 powder was purchased from Sigma-Aldrich (99.9%, -325 mesh) and used as received. First, 1.0 g the Nb_2O_5 powder was dissolved into a mixed solution of ethyl alcohol (60 mL) and distilled water (60 mL). Subsequently, 8 mM NH_4VO_3 (Sigma-Aldrich, 99%) and 24 mM $LiOH{\cdot}H_2O$ (Samchun, 98%) were dissolved in the solution. The solutions were placed in a Teflon-lined steel autoclave, heated to 120 ºC and maintained at that temperature for 12 h to induce hydrothermal reaction. After several washes with distilled water and ethyl alcohol, the precipitates were dried and annealed at 400 ºC for 2 h in an electrical furnace under pure nitrogen atmosphere. Subsequently, the furnace was automatically cooled down to room temperature.

2.2 Materials characterization

Crystalline structures of the prepared materials were identified through X-ray diffraction (XRD) using the Rigaku D/MAX-2500 with Cu Kα radiation. Field-emission scanning electron microscopy (FE-SEM, JEOL 7500) and high-resolution transmission electron microscopy (HR-TEM, JEOL ARM-200F) with an energy dispersive spectroscopy (EDS) detector were employed to characterize the morphologies, crystallinity, and elemental distribution of the synthesized samples. X-ray photoelectron spectroscopy (XPS, Thermo Scientific Kα) was adopted to determine the surface chemical states of the samples.

2.3 Electrochemical measurements

The working electrodes were prepared by coating a slurry comprising the synthesized active material (80 wt%), a conducting agent (10 wt%, Super P, Sigma-Aldrich), and a binder (10 wt%, polyacrylic acid, Sigma-Aldrich) onto Cu foil current collectors and dried at 80 ºC for 3 h. Then, the electrode was pressed by a roll-presser and vacuum-dried for 12 h. Subsequently, the electrode was cut into a disc with a diameter of 10 mm and used as a working electrode. Li metal foil was employed as the counter/reference electrode, and the electrolyte comprised 1.0 M $LiPF_6$ in ethylene carbonate and dimethyl carbonate (3:7 by volume ratio) along with 10 wt% fluoroethylene carbonate; porous polyethylene separators were also used. Coin-type 2032 half-cells were assembled in an Ar-filled glove box to characterize the electrochemical properties. Cycling experiments were galvanostatically performed using a battery tester (Basytec CTS-Lab) in the potential range of 0.01-3.0 V (vs. Li^+/Li) at 25 ºC . Rate capability was measured at various specific currents under the same conditions.

3. Results and Discussion

Fig. 1 displays the XRD patterns of the synthesized material with references. All observed diffraction peaks could be indexed to two phases of orthorhombic Li_3VO_4 (JCPDS No. 38-1247) and orthorhombic Nb_2O_5 (JCPDS No. 27-1402). This indicates that the Li_3VO_4 phase was synthesized without impurities through hydrothermal reaction and annealing. The composite is expected to

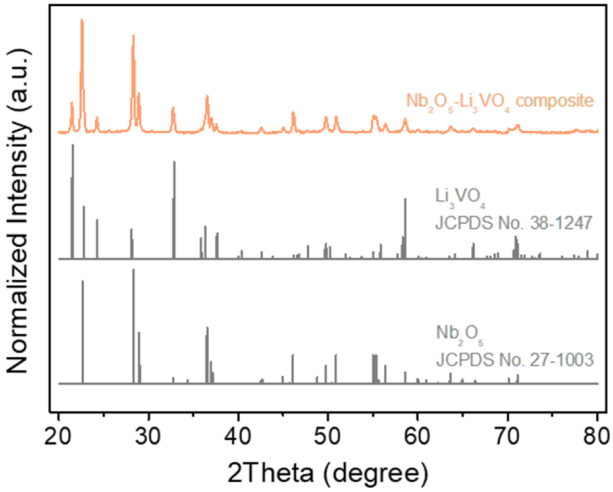

Fig. 1. XRD patterns of the synthesized material along with references

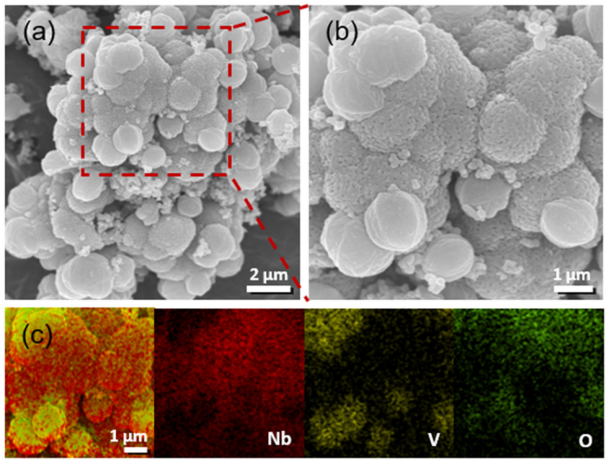

Fig. 2. (a,b) FE-SEM images and (c) the corresponding EDS elemental mapping results of the Nb_2O_5-Li_3VO_4 composite

comprise starting Nb_2O_5 and synthesized Li_3VO_4. The morphology of the sample was examined using FE-SEM. Fig. 2a and b display the FE-SEM images of the Nb_2O_5-Li_3VO_4 composite. The spherically shaped particles measuring a few microns were observed to be agglomerated. The corresponding EDS elemental mapping results are shown in Fig. 2c. The signals for Nb and V were inversely detected, indicating that primary Nb_2O_5 and Li_3VO_4 particles are mixed in the composite.

Fig. 3 presents the TEM analysis results for the composite. Fig. 3a and b display the low- and high-magnification TEM images of the composite particles, which were enlarged to obtain several HR-TEM images. Two typical HR-TEM images along with fast Fourier transform (FFT) patterns (inset) are shown in Fig. 3c and d. Well-crystallized Nb_2O_5 domains were observed and the corresponding d-spacing of 3.14 Å could be attributed to the (180) reflection plane of orthorhombic Nb_2O_5 (Fig. 3c), which was confirmed in the FFT pattern [11]. Fig. 3d displays another HR-TEM image wherein a crystalline domain was observed with a different d-spacing of 4.13 Å, which could be matched with the (110) reflection of orthorhombic Li_3VO_4 [12]. The inset FFT pattern also confirmed the existence of the Li_3VO_4 phase. The TEM image shown in Fig. 3a was analyzed using EDS elemental mapping, the results of which are shown in Fig. 3e. The O element was observed in the entire particle composite, whereas Nb and V elements were inversely located. This observation corresponds well to the EDS

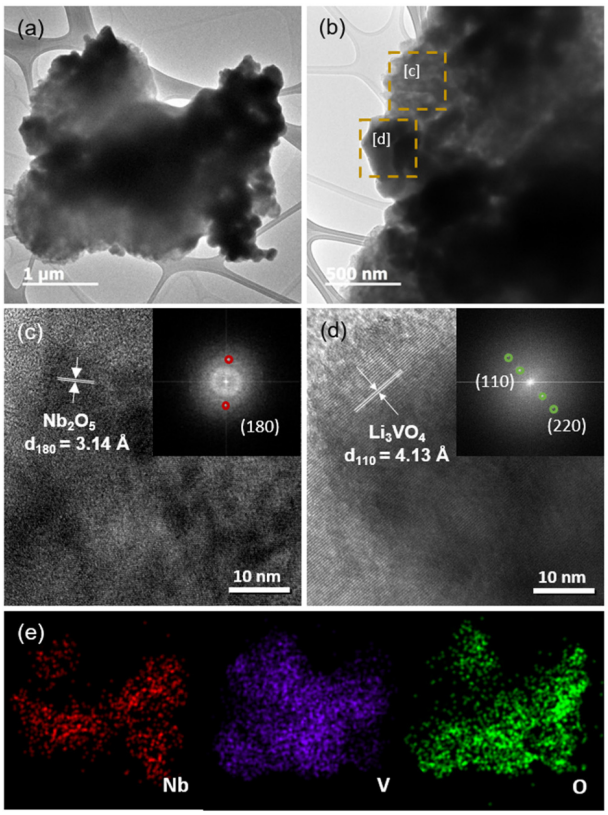

Fig. 3. (a, b) TEM images, (c, d) HR-TEM images (inset: FFT pattern), and (e) EDS elemental mapping results of the Nb_2O_5-Li_3VO_4 composite

elemental mapping results in the FE-SEM image (Fig. 2c).

The chemical states of the composites were examined using XPS. The surface of the sample was cleaned using Ar-ion etching for 300 s. Fig. 4a displays the XPS V 2p core-level spectrum for the Nb_2O_5-Li_3VO_4 composite with peaks corresponding to the 2p1/2 and 2p3/2 orbitals of V. The peaks were deconvoluted into two major sub-profiles centered at 524.7 and 516.8 eV that represented V in its pentavalent state (V^{5+}) with its oxidation number corresponding to the Li_3VO_4 phase [13,14]. Small sub-profiles at 523.0 and 516.8 eV represented the tetravalent state of V (V^{4+}). These results indicated that some oxygen vacancies may still exist in the material [14]. The Nb 3d core-level spectrum of the composite sample with deconvoluted sub-profiles is shown in Fig. 4b. The binding energy distribution was similar to that of V with sub-profiles centered at 210.4 and 207.6 eV representing the Nb^{5+} oxidation state, as previously reported [11,15]. Very small sub-profiles observed at 209.0 and 206.1 eV are ascribed to Nb^{4+} state [15]. All these features originate

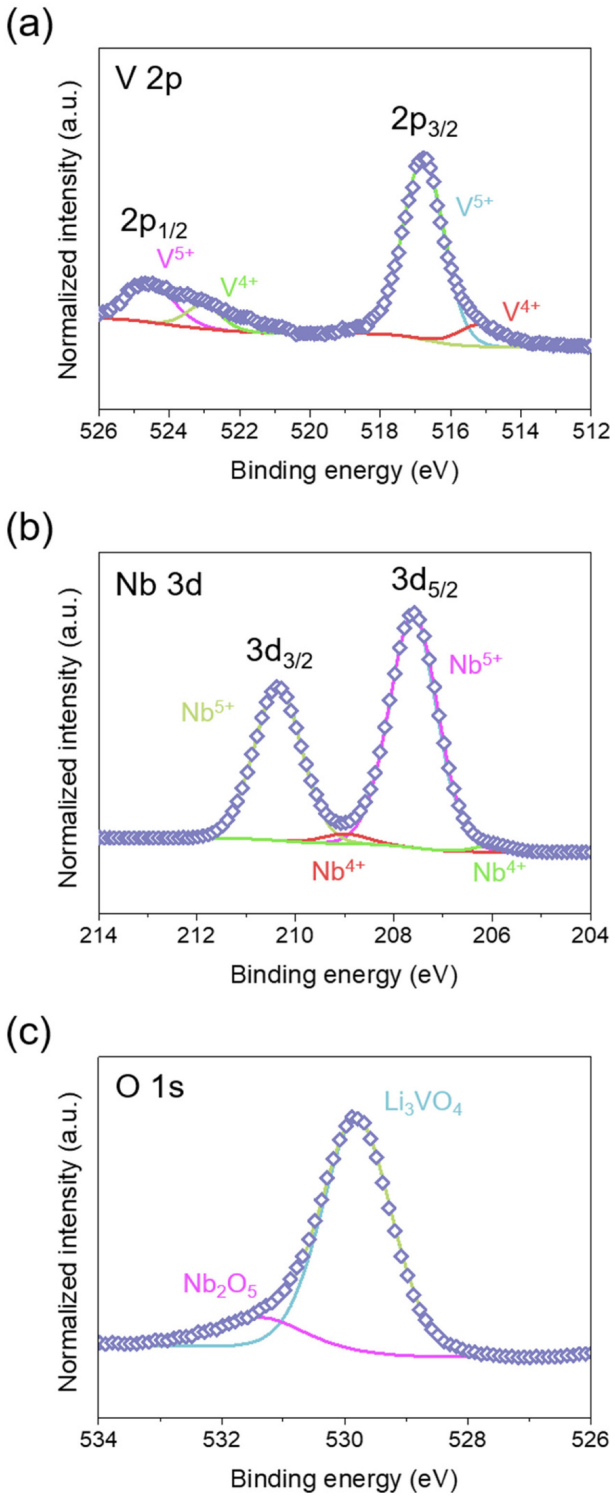

Fig. 4. XPS core-level spectra of the Nb_2O_5-Li_3VO_4 composite: (a) V 2p, (b) Nb 3d, and (c) O 1s

from the orthorhombic Nb_2O_5 phase in the composite. The O 1s core-level spectrum is shown in Fig. 4c. The spectrum was deconvoluted into two sub-profiles centered at 531.5 and 529.8 eV, corresponding to the O in Nb_2O_5 and Li_3VO_4, respectively [11,13]. All these XPS analysis results revealed that the Nb_2O_5 and Li_3VO_4 phases are mixed in the composite.

Fig. 5a displays the voltage profiles for the first two cycles of the Nb_2O_5-Li_3VO_4 composite electrode that were measured at a constant specific current of 50 mA g^{-1}. The discharge (Li insertion) and charge (Li extraction) capacities were 528 and 353 mAh g^{-1}, respectively, with an initial Coulombic efficiency of 66.8%. The sloped portion between 2.0 and 1.0 V vs. Li^+/Li during discharge could be associated with the Li insertion into the Nb_2O_5 phase, as previously reported [16,17]. Furthermore, solid electrolyte interphase (SEI) layer formation could occur in the region. Below 1.0 V, the Li can be inserted into the Li_3VO_4, as previously reported [18,19]. During charging, Li would be sequentially extracted from Li_3VO_4 and Nb_2O_5.

Fig. 5b shows the cycle performance of the Nb_2O_5-Li_3VO_4 composite electrode measured at 50 mA g^{-1}. A reversible capacity of more than 300 mAh g^{-1} could be maintained for up to 100 cycles. This robust cycling stability can be attributed to the microstructure of the composite. The Nb_2O_5 and Li_3VO_4 particles are mixed and well attached to each other in the composite, which can buffer the volume change of both materials during Li insertion and extraction cycling. Long-term cycle performance at a high rate of 5 C (1.5 A g^{-1}, 1 C = 300 mAh g^{-1}) is shown in Fig. 5c. In the first stage, the reversible capacity increased gradually with an increase in cycle number. This phenomenon can be related to the activation of the electrode materials because the cycling current was very high. After 100 cycles, the capacity reached approximately 140 mAh g^{-1} and was maintained well for up to 1000 cycles. In our previous study [20], a carbon-coated Nb_2O_5 nanoparticle electrode exhibited a reversible capacity of approximately 100 mAh g^{-1} after 1000 cycles at a rate of 5 C (1.0 A g^{-1}, 1 C = 200 mAh g^{-1} for Nb_2O_5). In comparison, the Nb_2O_5-Li_3VO_4 composite electrode fabricated here demonstrated a much higher capacity at a high specific current (1.5 A g^{-1}). This result could be attributed to fast Li ion transport caused by the high Li ion conduction in the Li_3VO_4 phase. Moreover, the Li_3VO_4 phase can store more Li ions through insertion reactions.

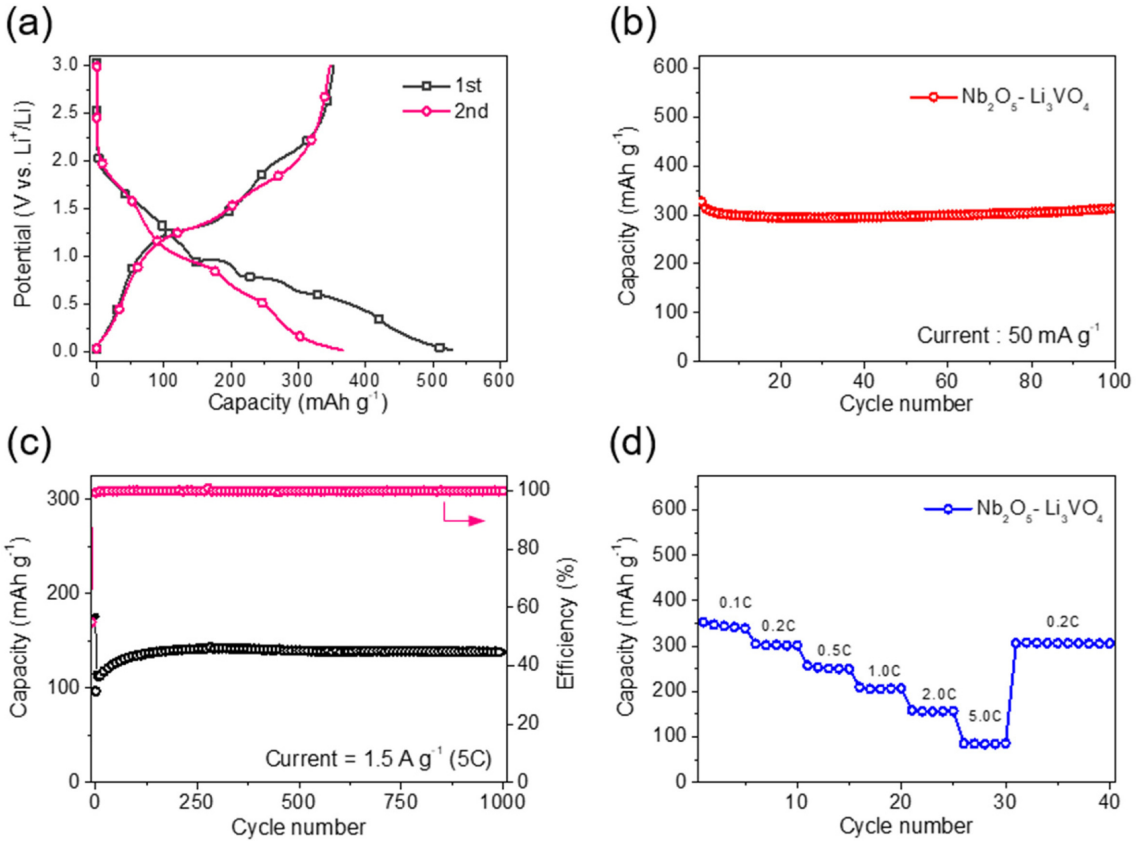

Fig. 5. Electrochemical properties of the Nb_2O_5-Li_3VO_4 composite electrode: (a) voltage profiles at 50 mAh g^{-1}, (b) cycle performance at 50 mAh g^{-1}, (c) long-term cycle performance at 1.5 A g^{-1} (5 C), and (d) rate performance

Fig. 5d presents the rate performance of the Nb_2O_5-Li_3VO_4 composite electrode at varying rates of 0.1–5 C. The electrode exhibited a reversible capacity of about 350 and 210 mAh g^{-1} at 0.1 and 1 C, respectively. The capacity of the composite at 1 C was higher than those of pure or C-coated Nb_2O_5 materials [20], which reveals that the synthesized composite electrode has some potential for mid- and/or high-rate Li-storage applications.

4. Conclusions

An Nb_2O_5-Li_3VO_4 composite was prepared as an anode material for LIBs and hybrid supercapacitors. Nb_2O_5 powders were first dissolved into a solution and then the precursors were precipitated onto the Li_3VO_4 through simple low-temperature hydrothermal reaction. After annealing, the Nb_2O_5-Li_3VO_4 composite was successfully synthesized. The formation of Li_3VO_4 was confirmed by XRD and XPS. The morphology was observed using FE-SEM and TEM; EDS elemental mapping results revealed the distribution of each element. The electrochemical test revealed that the Nb_2O_5-Li_3VO_4 composite electrode had an increased capacity of approximately 350 mAh g^{-1}, compared to that of Nb_2O_5, as well as good cycle and rate performance that can be ascribed to the microstructure design of the synthesized composite material.

Acknowledgments

This work was supported by the National Research Foundation of Korea (NRF) Grant funded by the Korean Government (2015R1A5A7037615 and 2019R1F1A1062835).

References

1. M. Winter, J. O. Besenhard, M. E. Spahr, and P. Novák, Insertion Electrode Materials for Rechargeable Lithium

Batteries, *Advanced Materials*, **10**, 725 (1998). Doi: https://doi.org/10.1002/(SICI)1521-4095(199807)10:10<725::AID-ADMA725>3.0.CO;2-Z

2. M. Winter and R. J. Brodd, What Are Batteries, Fuel Cells, and Supercapacitors?, *Chemical Reviews*, ***104***, 4245 (2004). Doi: https://doi.org/10.1021/cr020730k
3. S. J. Hong, S. S. Kim, and S. Nam, Using Coffee-Derived Hard Carbon as a Cost-Effective and Eco-Friendly Anode Material for Li-Ion Batteries, *Corrosion Science and Technology*, **20**, 15 (2021). Doi: https://doi.org/10.14773/CST.2021.20.1.15
4. K. Kim, H.-S. Kim, H. Seo, and J.-H. Kim, Electrochemical and Thermal Property Enhancement of Natural Graphite Electrodes via a Phosphorus and Nitrogen Incorporating Surface Treatment, *Corrosion Science and Technology*, **19**, 31 (2020). Doi: https://doi.org/10.14773/CST.2020.19.1.31
5. M. N. Obrovac and V. L. Chevrier, Alloy Negative Electrodes for Li-Ion Batteries, *Chemical Reviews*, **114**, 11444 (2014). Doi: https://doi.org/10.1021/cr500207g
6. B. Zhao, R. Ran, M. Liu, and Z. Shao, A comprehensive review of $Li_4Ti_5O_{12}$-based electrodes for lithium-ion batteries: The latest advancements and future perspectives, *Materials Science and Engineering R*, **98**, 1 (2015). Doi: https://doi.org/10.1016/j.mser.2015.10.001
7. Y. Zhang, Y. Tang, W. Li, and X. Chen, Nanostructured TiO_2-Based Anode Materials for High-Performance Rechargeable Lithium-Ion Batteries, *ChemNanoMat*, **2**, 764 (2016). Doi: https://doi.org/10.1002/cnma.201600093
8. F. Shen, Z. Sun, Q. He, J. Sun, R. B. Kaner, and Y. Shao, Niobium pentoxide based materials for high rate rechargeable electrochemical energy storage, *Materials Horizons*, **8**, 1130 (2021). Doi: https://doi.org/10.1039/D0MH01481H
9. L. Yan, X. Rui, G. Chen, W. Xu, G. Zou, and H. Luo, Recent advances in nanostructured Nb-based oxides for electrochemical energy storage, *Nanoscale*, **8**, 8443 (2016). Doi: https://doi.org/10.1039/C6NR01340F
10. H. Li, X. Liu, T. Zhai, D. Li, and H. Zhou, Li_3VO_4: A Promising Insertion Anode Material for Lithium-Ion Batteries, *Advanced Energy Materials*, **3**, 428 (2013). Doi: https://doi.org/10.1002/aenm.201200833
11. K. Kim and J.-H. Kim, Bottom-up self-assembly of nanonetting cluster microspheres as high-performance lithium storage materials, *Journal of Materials Chemistry A*, **6**, 13321 (2018). Doi: https://doi.org/10.1039/C8TA04851G
12. J. Zeng, Y. Yang, C. Li, J. Li, J. Huang, J. Wang, and J. Zhao, Li_3VO_4: an insertion anode material for magnesium ion batteries with high specific capacity, *Electrochimica Acta*, **247**, 265 (2017). Doi: https://doi.org/10.1016/j.electacta.2017.06.143
13. E. Thauer, G. S. Zakharova, S. A. Wegener, Q. Zhu, and R. Klingeler, Sol-gel synthesis of Li_3VO_4/C composites as anode materials for lithium-ion batteries, *Journal of Alloys and Compounds*, **853**, 157364 (2021). Doi: https://doi.org/10.1016/j.jallcom.2020.157364
14. J. Zhou, B. Zhao, J. Song, B. Chen, X. Ma, J. Dai, X. Zhu, and Y. Sun, Optimization of Rate Capability and Cyclability Performance in Li_3VO_4 Anode Material through Ca Doping, *Chemistry A European Journal*, **23**, 16338 (2017). Doi: https://doi.org/10.1002/chem.201703405
15. K. Kim, M.-S. Kim, P.-R. Cha, S. H. Kang, J.-H. Kim, Structural Modification of Self-Organized Nanoporous Niobium Oxide via Hydrogen Treatment, *Chemistry of Materials*, **28**, 1453 (2016). Doi: http://doi.org/10.1021/acs.chemmater.5b04845
16. J. W. Kim, V. Augustyn, B. Dunn, The Effect of Crystallinity on the Rapid Pseudocapacitive Response of Nb_2O_5, *Advanced Energy Materials*, **2**, 141 (2012). Doi: https://doi.org/10.1002/aenm.201100494
17. J. Come, V. Augustyn, J. W. Kim, P. Rozier, P.-L. Taberna, P. Gogotsi, J. W. Long, B. Dunn, and P. Simon, Electrochemical Kinetics of Nanostructured Nb_2O_5 Electrodes, *Journal of The Electrochemical Society*, **161**, A718 (2014). Doi: https://doi.org/10.1149/2.040405jes
18. C. Liao, Y. Wen, B. Shan, T. Zhai, andH. Li, Probing the capacity loss of Li_3VO_4 anode upon Li insertion and extraction, *Journal of Power Sources*, **348**, 48 (2017). Doi: https://doi.org/10.1016/j.jpowsour.2017.02.075
19. Z. Liang, Z. Lin, Y. Zhao, Y. Dong, Q. Kuang, X. Lin, X. Liu, and D. Yan, New understanding of Li_3VO_4/C as potential anode for Li-ion batteries: Preparation, structure characterization and lithium insertion mechanism, *Journal of Power Sources*, **274**, 345 (2015). Doi: https://doi.org/10.1016/j.jpowsour.2014.10.024
20. K. Kim, S.-G. Woo, Y. N. Jo, J. Lee, and J.-H. Kim, Niobium oxide nanoparticle core–amorphous carbon shell structure for fast reversible lithium storage, *Electrochimica Acta*, **240**, 316 (2017). Doi: https://doi.org/10.1016/j.electacta.2017.04.051